Research Square

Preprints are preliminary reports that have not undergone peer review.
They should not be considered conclusive, used to inform clinical practice,
or referenced by the media as validated information.

Cerebral Functional Reorganization Associated with Spinal Structural Injury Severity in Cervical Spondylotic Myelopathy

Shuting Huang
Tongji Hospital, Tongji Medical College, Huazhong University of Science and Technology
Longyu Deng
Tongji Hospital, Tongji Medical College, Huazhong University of Science and Technology
Qiya Zhang
Eighth Affiliated Hospital of Sun Yat-sen University
Weiyin Vivian Liu
Bayer Healthcare
Chaoxu Liu
Tongji Hospital, Tongji Medical College, Huazhong University of Science and Technology
Xiangyu Tang
tangxiangyude@163.com
Tongji Hospital, Tongji Medical College, Huazhong University of Science and Technology
Wenzhen Zhu
Tongji Hospital, Tongji Medical College, Huazhong University of Science and Technology

Research Article

Keywords: Cervical spondylotic myelopathy, Resting-state functional magnetic resonance imaging, fALFF, Functional connectivity

Posted Date: April 19th, 2026

DOI: https://doi.org/10.21203/rs.3.rs-8978406/v1

License: This work is licensed under a Creative Commons Attribution 4.0 International License.
Read Full License

Additional Declarations: No competing interests reported.

Abstract

Purpose: To investigate the impact of spinal cord injury severity on thalamus-cortical functional reorganization in patients with cervical spondylotic myelopathy (CSM).

Methods: All subjects (66 CSM patients and 43 healthy controls) underwent brain resting-state functional MRI (rs-fMRI) and spinal synthetic MRI. CSM patients were subdivided into non-high-signal (CSM-nonHS, n = 41) and high-signal (CSM-HS, n = 25) groups based on the spinal intensity on T2WI. Z-scored functional connectivity (zFC) with the ventral posterolateral nucleus (VPL) as seed regions and whole-brain z-scored fractional amplitude of low-frequency fluctuations(zfALFF) values were computed and compared among groups. Mean zFC and zfALFF values from regions showing group differences were extracted for correlation analyses with quantitative spinal cord metrics [T1, T2 and proton density (PD) values] and clinical scores [Visual Analog Scale (VAS) for pain and Japanese Orthopaedic Association (JOA) score].

Results: Compared with healthy controls, zFC between the left VPL and the right postcentral gyrus, middle cingulate cortex, and paracentral lobule was enhanced in CSM-nonHS group but markedly diminished in the CSM-HS group. Both CSM subgroups showed increased zfALFF in left precentral gyrus and paracentral lobule. Furthermore, the mean VPL-sensory cortex zFC negatively correlated with spinal cord T1 and T2 values, while positively correlating with JOA scores. The mean zfALFF in the motor cortex correlated positively with PD values.

Conclusion: CSM patients exhibit characteristic functional alterations in thalamus and sensorimotor cortex, which are dependent on the severity of spinal cord injury. These findings provide novel insights into the adaptive reorganization and potential maladaptive disintegration mechanisms following chronic spinal cord compression.

Clinical trial registration: Not applicable (observational study).

1. Introduction

Cervical spondylotic myelopathy (CSM), the most common spinal cord impairment, is characterized by chronic progressive compression of the cervical cord due to degenerative disc disease, spondylosis, or other degenerative pathology[1]. While prior research has predominantly focused on local spinal cord injury[2, 3], emerging evidence indicates that CSM can also induce noticeable alterations in brain structure [4], function[5, 6], and connectivity[7]. These supraspinal changes may exacerbate clinical symptoms and affect recovery processes. However, the relationship between the extent of cerebral functional reorganization level and the severity of spinal injury remains unclear.

Resting-state functional magnetic resonance imaging (rs-fMRI) is frequently used to evaluate functional plasticity. A recent study using the primary motor cortex as a priori region of interest (ROI) revealed that the CSM patients with more severe clinical symptoms exhibited higher amplitude of

low-frequency fluctuations (ALFF) in this region, indicating a contribution of cortical function to clinical severity[8]. Furthermore, the thalamus, as a critical relay station between the spinal cord and the cerebral cortex plays an essential role in regulating sensorimotor information[9]. However, current researches on thalamocortical connectivity has primarily focus on acute spinal cord injury models[10, 11], investigations in CSM remain limited and existing results are controversial[12, 13].

In this study, we subdivided CSM patients into non-high-signal (CSM-nonHS) and high-signal (CSM-HS) groups based on the spinal intensity on T2-weight images to compare the seed-based functional connectivity analysis (SCA) and fractional ALFF across groups. Furthermore, we employed synthetic MRI to quantitatively evaluate the relationship between spinal cord relaxation parameters and cerebral functional reorganization level in CSM[14], since the relaxation times are frequently associated with significant pathological changes such as ischemia, edema, gliosis, myelomalacia or demyelination [15, 16], with increased T1 and T2 value often indicating more severe spinal injury and a less favorable prognosis[17].

Therefore, we employed two complementary rs-fMRI metrics, fALFF and thalamocortical functional connectivity, to investigate cerebral functional reorganization in CSM. We hypothesized that the degree of this reorganization is related to the spinal injury severity.

2. Materials and Methods

2.1 Subjects and Clinical assessment

This study was approved by the institutional review board on May 24, 2022 (TJ-IRB20220558). Written informed consent was obtained from all participated. From August 2022 to May 2025, 112 right-handed subjects were initially enrolled. Three subjects were excluded due to excessive head motion during fMRI acquisition. This final cohort consisted of 43 healthy controls (HCs) and 66 patients with CSM caused by cervical disc herniation. Clinical evaluation included the Japanese Orthopedic Association (JOA) score to assess myelopathy severity and a 10-cm visual analogue scale (VAS) for pain intensity. Subjects were classified into three groups: 1) Healthy controls (HC): No or mild spinal canal stenosis without cord compression; 2) CSM-nonHS group: Radiographic spinal cord compression without T2-weighted hyperintensity; 3) CSM-HS: Spinal cord compression with T2-weighted hyperintensity at/near the compressed level.

Exclusion criteria comprised: 1) Neurologic, psychiatric, or systemic illness unrelated to CSM; 2) History of brain or cervical spine surgery; 3) Musculoskeletal disorders affecting extremity sensorimotor function; 4) Standard MRI contraindications (e.g., metal implants, claustrophobia).

2.2 Image acquisition

MRI scans were performed on a 3.0-Tesla scanner (Premier, GE Healthcare, Milwaukee, USA) with a 21-channel head and neck coil. All subjects were instructed to remain still, awake, and eyes closed during

the scanning procedure. Conventional sagittal and axial fat-saturated T2-weighted fast spin-echo sequences were acquired for grading and morphometry. BOLD data were acquired using a gradient-echo-planar imaging (GRE-EPI) sequence: TR/TE= 2000/30 ms, FOV = 240 × 240 mm^2, matrix size=80×80, flip angle=90◦, slice thickness=3 mm (no gap), 160 volumes, scanning time = 8 min. High-resolution 3D T1-weighted structural images were obtained using a brain volume sequence: TR/TE = 7.2/2.9 ms, flip angle=12°, FOV = 280×100 mm^2, matrix size=256 × 256, slice thickness =1 mm (no gap), 156 sagittal slices, scanning time=2 minutes and 47 seconds. Synthetic MRI parameters were as follows: TR/TE=4008 /29.3 ms, slice thickness=4 mm, spacing=1.0 mm, field of view (FOV)=240×192 mm2, NEX=1.00, scanning time=7 minutes and 45 seconds. One healthy control and four patients did not complete synthetic MRI scanning.

4 Spinal cord data processing

The degree of spinal cord compression and signal changes for all subjects was independently assessed by two senior experienced radiologists, with a decision made by consensus. The maximum spinal cord compression (MSCC) ratio was assessed on midsagittal T2WI employing a validated method [18]. Synthetic MRI data were processed using SyMRI software (v11.2.2, SyntheticMR, Linköping, Sweden) to generate quantitative T1, T2, and proton density (PD) maps **(Fig 1)**. ROIs were manually delineated at the maximal compression level (MCL) on a synthetic T2WI maps, and the corresponding T1, T2 and PD values were extracted.

2.4 fMRI preprocessing and analysis

The functional MRI data were preprocessed with SPM12 (http://dbm.neuro.uni-jena.de/vbm/) and the DPABI toolbox(http://rfmri.org/dpabi). The steps included: 1) The initial 10 volumes were discarded to allow for magnetic stabilization. 2) Slice-timing correction and realignment were applied to compensate for acquisition time delays and head motion, respectively. Head motion >3 mm translation or >3° rotation were excluded; 3) The functional images were co-registered to the structural images, spatially normalized into the Montreal Neurological Institute (MNI) space using diffeomorphic anatomical registration through the exponentiated Lie algebra (DARTEL) and resampled to 3 × 3 × 3 mm^3. 4) All data underwent nuisance covariate regression (Friston-24 head motion parameters, white matter signals, and cerebrospinal fluid signals) and linear detrending. 5) Spatial smoothing was utilized using a Gaussian kernel with a full width at half maximum (FWHM) of 6mm.

zfALFF calculation: Time series were transformed to the frequency domain. The fALFF was calculated as the ratio of power in the 0.01-0.08 Hz band to that in the full frequency range (0-0.25 Hz). Voxel-wise fALFF maps were then z-scored to produce zfALFF maps.

Thalamus-cortex zFC calculation: Using the automated anatomical labeling atlas 3, the bilateral ventral posterolateral nucleus (VPL) was selected as the seed ROIs, given its role in relaying somatic sensory information from the trunk and limbs and its relevance to CSM-related sensory impairment[19]. ROIs masks were created the MARSBAR toolbox (http://www.marsbar.sourceforge.net). Functional

connectivity was assessed by computing the Pearson correlation coefficient between the mean resting-state time series of each seed ROI and the time series of all other brain voxels. with Fisher's z transformation. These individual FC maps were further normalized via z-score transformation across the whole brain to produce final zFC maps for group-level analysis.

Mean zfALFF and zFC values from brain regions exhibiting differences among the three groups were extracted for subsequent post hoc tests and correlation analysis.

2.4 Statistical analysis

Data were represented as mean and standard deviation SD. Group comparisons of zfALFF and zFC maps were performed using One-way ANOVA in SPM12, with age, sex, and education as covariates. Statistical significance was set at a cluster-level family-wise (FWE) with initial voxel-wise threshold $p < 0.001$, corrected $p<0.05$. Extracted mean values underwent Bonferroni-corrected post-hoc tests.

Demographics and correlations were analyzed using SPSS software (IBM, Armonk, NY). Continuous variables (ages, years of education, VAS scores, synthetic MRI metrics) were compared using Kruskal-Wallis test; JOA scores and MSCC rates with the Mann–Whitney U test. Categorical data (gender) were compared using the χ^2 test. Spearman's rank correlation assessed correlations between spinal metrics, clinical scores, and fMRI indices. Inter-observer reliability for quantitative measurements was evaluated using intraclass correlation coefficients (ICC).

3. Results

3.1 Demographic and Clinical characteristics

The final cohort comprised 66 CSM patients and 43 healthy controls. CSM patients were subdivided into a non-high-signal group (CSM-nonHS; n = 41; 20 males, mean age 51.5±10.4 years) and a high-signal group (CSM-HS; n = 25; 16 males; mean age 50.7±9.4 years). Demographic data are summarized in **Table 1**. No significant difference was observed among three groups in age, gender, and years of education. Compared to CSM-nonHS group, the CSM-HS group had significantly lower JOA scores ($p<0.001$), as well as lower motor ($p=0.009$) and sensory subscores ($p<0.001$). No significant difference in VAS scores was found between the two CSM subgroups ($p=0.39$).

Table 1. Demographics and clinical characteristics of healthy controls (HCs) and patients with cervical spondylotic myelopathy (CSM).

Variables	CSM-nonHS	CSM-HS	HC	P value
	(n=41)	(n=25)	(n=43)	
Sex (male/female)	20/21	16/9	21/22	0.41
Age (years)	51.5±10.4	50.7±9.4	46.9±8.9	0.08
Education (years)	13.2±3.3	13.0±2.8	14.1±2.9	0.12
VAS	3.2±2.34	3.48±1.90	0.88±0.88	<0.001*, †
JOA scores (Total)	14.59±1.87	12.84±1.75	N/A	<0.001
Motor scores	7.05±1.20	6.36±1.04	N/A	0.009
Sensory scores	4.56±1.10	3.52±0.96	N/A	<0.001
Bladder function	2.98±0.16	2.96±0.20	N/A	0.72

Note: Data are presented as mean ± standard deviation unless otherwise indicated. CSM-nonHS: CSM patients without high signal on T2WI. CSM-HS: CSM patients with high signal on T2WI. JOA: Japanese Orthopaedic Association; VAS: Visual Analog Scale. Post hoc comparisons: *, HC vs CSM-nonHS; †, HC vs CSM-HS

3.2 Comparison of thalamus-cortex zFC

Group-level analysis revealed significant differences in zFC between the left VPL and a cluster encompassing the right postcentral gyrus, middle cingulate cortex, paracentral lobule, and precuneus gyrus ($p_{cluster\text{-}FWE}$ <0.05; **Table 2, Fig 2a)**. Analysis of the extracted mean connectivity strengths showed that the CSM-nonHS group exhibited increased zFC compared with HCs (p=0.02). In contrast, the CSM-HS showed significantly reduced zFC compared to CSM-nonHS and HCs (p=0.01 and p<0.001, respectively, **Fig 2b)**. No significant difference in zFC were observed for the right VPL seed among three groups.

Table 2. Brain regions of significant group difference in z-scored functional connectivity (zFC) with the left ventral posterolateral nucleus.

Brain regions (AAL)	Voxels	Peak MNI			F value
		x	y	z	
Cluster 1	87	21	-36	54	13.37
Right Postcentral Gyrus	41				
Right Middle Cingulum	25				
Right Paracentral Lobule	20				
Right Precuneus Gyrus	1				

3.3 Comparison of zfALFF

Significant group differences in zfALFF were identified in the left precentral gyrus and paracentral lobule ($p_{cluster\text{-}FWE}$ <0.05; **Table 3, Fig 3a)**. Post-hoc analysis of the extracted mean zfALFF values demonstrated that both the CSM-nonHS (p=0.01) and CSM-HS (p<0.001) groups had significantly higher zfALFF compared to HCs. The mean zfALFF values exhibited an upward trend in the CSM-HS group compared to the CSM-nonHS group although there was no significant difference between the two CSM subgroups **(Fig 3b)**.

Table 3. Brain regions of significant group differences in z-scored fractional amplitude of low-frequency fluctuations (zfALFF).

Brain regions (AAL)	Voxels	Peak MNI			F value
		x	y	z	
Cluster 1	19	-15	-12	78	10.26
Left Precentral Gyrus	12				
Left Paracentral Lobule	7				

3.4 Quantitative spinal cord metrics and their correlations with rs-fMRI indicators

Inter-observer consistencies (ICCs) for all spinal cord measurements were excellent (ICCs range: 0.935-0.981). At the MCL, T1 and T2 values were significantly higher in CSM-HS group than in CSM-nonHS group (p<0.001). The PD_{MCL} value was significantly higher in CSM-HS group than HCs (p=0.01) but did not differ significantly between CSM-nonHS group and either the CSM-HS group or HCs **(Table4)**.

The extracted mean FC strength negatively correlated with the MSCC ratio (p=0.003, r=-0.356), $T1_{MCL}$ (p= 0.005, r=-0.349), and $T2_{MCL}$ (P=0.004, r=-0.365) values, respectively **(Fig 4a-c)**. The mean motor cortex

zfALFF correlated positively only with PD_{MCL} values (p<0.001, r=0.419) and showed no significant correlation with other spinal quantitative parameters. **(Fig 4d)**.

Table 4. Quantitative spinal cord parameters at maximum compression level (MCL) in CSM patients and healthy controls (HCs).

Variables	CSM-nonHS	CSM-HS	HC	P value
MSCC (%)	14.50±6.91	30.37±16.52	N/A	<0.001‡
$T1_{MCL}$ value(ms)	1140.1±155.8	1394.0±251.5	1225.1±144.0	<0.001*‡
$T2_{MCL}$ value(ms)	87.7±4.1	93.2±4.8	88.6±3.9	<0.001†,‡
PD_{MCL} value(pu)	79.6±6.8	84.1±7.2	78.4±6.4	0.01†

Note: Data are presented as mean ± standard deviation. MSCC: maximum spinal cord compression; PD: proton density; pu: proton density arbitrary units. Post hoc comparisons: *, HC vs CSM-nonHS; †, HC vs CSM-HS; ‡, CSM-nonHS vs CSM-HS.

3.5 Association between clinical scores and rs-fMRI indictors

The mean zFC strength between the left VPL and the right postcentral gyrus, middle cingulate cortex, and paracentral lobule correlated positively with total JOA scores (p=0.016, r=0.296) and JOA sensory subscores (p=0.003, r=0.359) **(Fig 5a-b)**, while mean zfALFF in the left precentral gyrus and paracentral lobule showed no significant correlation with JOA scores **(Fig 5e-g)**. Further, no significant correlation was observed between zFC, zfALFF and VAS scores (p=0.240 and p=0.478, respectively).

4. Discussion

This study employed complementary resting-state fMRI metrics, seed-based functional connectivity (FC) and fALFF, to investigate cerebral reorganization in CSM. By innovatively integrating these with quantitative spinal cord parameters from synthetic MRI, we examined the effects of chronic spinal cord injury on thalamocortical circuits. The principal findings indicated that the cerebral functional reorganization mainly occurred within sensorimotor networks. Specifically, thalamocortical connectivity demonstrated a bidirectional change and it correlated with spinal injury severity, while local motor cortex activity was elevated in both patient groups.

Using the VPL as a seed region, we observed non-unidirectional alterations in thalamocortical connectivity in CSM patients. The CSM-nonHS group exhibited enhanced connectivity between the left VPL and right-hemispheric sensory areas (right postcentral gyrus, middle cingulate gyrus, and paracentral lobule), whereas the CSM-HS group showed significantly reduced connectivity in the same network. These opposing changes may reflect two potential mechanisms: firstly, compensatory cortical recruitment and diminished inhibitory neuronal influence[13], leading to initial hyperconnectivity to offset

reduced sensory input, as in CSM-nonHS patients; Secondly, abnormal thalamic burst firing triggered by more severe spinal cord injury, which disrupts thalamocortical rhythmic synchronization and beyond a compensatory threshold, leading to thalamocortical disconnection, as in CSM-HS patients [20, 21]. This aligned with previous reports of reduced connectivity in animal models of spinal cord severe injury [11]. FC changes are predominantly observed in the right cortices, which may be attributed to the right-lateralization advantage in somatosensory processing in certain brain areas. This result was consistent with a previous functional imaging study on chronic neuropathic pain, which showed that patients with bilateral somatic pain exhibit activation only in the right cingulate gyrus (rather than the left)[22].

Our study revealed increased zfALFF in precentral gyrus and paracentral lobule in CSM patients aligns with previous research[8, 23]. This may reflect several adaptive mechanisms: cortical plasticity through disinhibition or axonal sprouting [24], structural hypertrophy in these regions [25, 26], or local rewiring at the cervical level [27]. The non-significant trend toward increase in patients with high signal intensity suggests ongoing, possibly compensatory, reorganization even with severe injury, analogous to findings in traumatic spinal cord injury [28]. The left lateralization of thalamus and motor cortex dysfunction is consistent with studying right-handed (or left hemisphere motor dominant) individuals [10].

Elevated T1 and T2 relaxation times as well as proton density often indicate more severe pathological processes such as spinal cord ischemia, inflammation, and demyelination [16, 29]. The strong negative correlation between VPL-sensory cortex connectivity and quantitative spinal injury markers underscores that the integrity of this thalamocortical pathway is tied to the severity of structural cord damage. It supports the concept that spinal pathology is a key driver of network-level disintegration. Furthermore, this study showed a specific positive correlation between zfALFF in primary motor cortex and PD values at the MCL, which indicated particular sensitivity of PD mapping to pathological changes in the corticospinal tract originating from this cortical region[30].

Clinically, the positive correlation between preserved VPL-sensory cortex zFC and better JOA scores suggests the sensory functional relevance of this pathway. The lack of correlation between motor cortex activity zfALFF and clinical scores indicates that increased zfALFF may represent a complex, non-linear adaptive response not directly proportional to clinical deficit, which aligned with previous studies[23, 31].

This study has several limitations. Firstly, the sample size in CSM-HS group was moderate, since conducting additional MRI examinations for severely symptomatic CSM-HS patients was quite difficult. In the future, we will enroll more CSM-HS patients to assess the impact of heterogeneity within the CSM-HS subgroup (e.g., variations in lesion morphology and location). Secondly, spinal cord ROIs encompassed the entire spinal cord at MCL without distinguishing specific sensory or motor tracts, as the distinction is difficult when the spinal signal alterations occur.

5. Conclusion

In patients with CSM, thalamus-sensory cortex functional connectivity exhibits bidirectional alteration, manifesting as augmentation or diminution dependent upon the severity of spinal cord structural injury.

The strength of this connectivity correlates with clinical symptom profiles. Concurrently, elevated zfALFF values in the primary motor cortex is observed in patients with more advanced injury. These findings provide mechanistic insights into the adaptive, and potentially maladaptive, reorganization of thalamocortical networks following chronic spinal cord compression and may contribute neuroimaging-based evidence for evaluating disease progression.

Abbreviations

CSM：Cervical Spondylotic Myelopathy; rs-fMRI：resting-state functional magnetic resonance imaging; zFC：z-scored functional connectivity; VPL：ventral posterolateral thalamic nucleus; zfALFF: z-scored fractional amplitude of low-frequency fluctuations; PD: proton density; MCL: maximum compression level; MSCC: maximum spinal cord compression; VAS: Visual Analog Scale; JOA: Japanese Orthopaedic Association; ROI：region of interest; BOLD: blood oxygen level-dependent; SCA: seed-based correlation analysis; GRE-EPI: gradient-echo-planar imaging; MNI: Montreal Neurological Institute; DARTEL: diffeomorphic anatomical registration through the exponentiated Lie algebra; FWHM: full width at half maximum; FWE: family-wise error; ICC: intraclass correlation coefficients

Declarations

Ethics approval: This study was performed in line with the principles of and with the 1964 Helsinki Declaration and its later amendments or comparable ethical standards and was granted by the Institutional Ethics Committee of Tongji Hospital, Tongji Medical College, Huazhong University of Science and Technology (May 24, 2022/No. 20220558). All subjects provided written informed consent prior to participation.

Funding: This work was supported by the National Natural Science Foundation of China (Grant No. 51907077).

Consent to participate: Informed consent was obtained from legal guardians.

Consent to publish：The authors affirm that human research participants signed informed consent regarding publishing their data and photographs.

Clinical trial registration: Not applicable (observational study).

References

1. Kalsi-Ryan S, Karadimas SK, Fehlings MG. Cervical spondylotic myelopathy: the clinical phenomenon and the current pathobiology of an increasingly prevalent and devastating disorder. Neuroscientist, 19(4)(2013), 409-21, https://doi.org/10.1177/1073858412467377
2. Haynes G, Muhammad F, Weber KA, 2nd, et al. Tract-specific magnetization transfer ratio provides insights into the severity of degenerative cervical myelopathy. Spinal Cord, 62(12)(2024), 700-7,

https://doi.org/10.1038/s41393-024-01036-y

3. Wen CY, Cui JL, Liu HS, et al. Is diffusion anisotropy a biomarker for disease severity and surgical prognosis of cervical spondylotic myelopathy? Radiology, 270(1)(2014), 197-204, https://doi.org/10.1148/radiol.13121885
4. Bernabéu-Sanz Á, Mollá-Torró JV, López-Celada S, et al. MRI evidence of brain atrophy, white matter damage, and functional adaptive changes in patients with cervical spondylosis and prolonged spinal cord compression. Eur Radiol, 30(1)(2020), 357-69, https://doi.org/10.1007/s00330-019-06352-z
5. Takenaka S, Kan S, Seymour B, et al. Resting-state Amplitude of Low-frequency Fluctuation is a Potentially Useful Prognostic Functional Biomarker in Cervical Myelopathy. Clin Orthop Relat Res, 478(7)(2020), 1667-80, https://doi.org/10.1097/corr.0000000000001157
6. Dong Y, Holly LT, Albistegui-Dubois R, et al. Compensatory cerebral adaptations before and evolving changes after surgical decompression in cervical spondylotic myelopathy. J Neurosurg Spine, 9(6)(2008), 538-51, https://doi.org/10.3171/spi.2008.10.0831
7. Xie B, Yao J, Ni H, et al. Dynamic functional network connectivity remodeling in cervical spondylotic myelopathy: insights into postoperative neural recovery. Spine J, 25(11)(2025), 2430-40, https://doi.org/10.1016/j.spinee.2025.04.003
8. Zhao R, Guo X, Wang Y, et al. Functional MRI evidence for primary motor cortex plasticity contributes to the disease's severity and prognosis of cervical spondylotic myelopathy patients. Eur Radiol, 32(6)(2022), 3693-704, https://doi.org/10.1007/s00330-021-08488-3
9. Biesbroek JM, Verhagen MG, van der Stigchel S, et al. When the central integrator disintegrates: A review of the role of the thalamus in cognition and dementia. Alzheimers Dement, 20(3)(2024), 2209-22, https://doi.org/10.1002/alz.13563
10. Karunakaran KD, Yuan R, He J, et al. Resting-State Functional Connectivity of the Thalamus in Complete Spinal Cord Injury. Neurorehabil Neural Repair, 34(2)(2020), 122-33, https://doi.org/10.1177/1545968319893299
11. Seminowicz DA, Jiang L, Ji Y, et al. Thalamocortical asynchrony in conditions of spinal cord injury pain in rats. J Neurosci, 32(45)(2012), 15843-8, https://doi.org/10.1523/jneurosci.2927-12.2012
12. Chang J, Zhu K, Zhang S, et al. Dysregulated neural activity between the thalamus and cerebral cortex mediates cortical reorganization in cervical spondylotic myelopathy. Brain Res Bull, 2052023), 110837, https://doi.org/10.1016/j.brainresbull.2023.110837
13. Zhou F, Wu L, Liu X, et al. Characterizing Thalamocortical Disturbances in Cervical Spondylotic Myelopathy: Revealed by Functional Connectivity under Two Slow Frequency Bands. PLoS One, 10(6)(2015), e0125913, https://doi.org/10.1371/journal.pone.0125913
14. Liu Q, Shao H, Liu C, et al. Quantitative evaluation of the spinal cord compression in patients with cervical spondylotic myelopathy using synthetic MRI. Front Physiol, 142023), 1140870, https://doi.org/10.3389/fphys.2023.1140870
15. Maier IL, Hofer S, Joseph AA, et al. Quantification of spinal cord compression using T1 mapping in patients with cervical spinal canal stenosis - Preliminary experience. Neuroimage Clin, 212019),

101639, https://doi.org/10.1016/j.nicl.2018.101639

16. Mastronardi L, Elsawaf A, Roperto R, et al. Prognostic relevance of the postoperative evolution of intramedullary spinal cord changes in signal intensity on magnetic resonance imaging after anterior decompression for cervical spondylotic myelopathy. J Neurosurg Spine, 7(6)(2007), 615-22, https://doi.org/10.3171/spi-07/12/615
17. Wang K, Chen Z, Zhang F, et al. Evaluation of DTI Parameter Ratios and Diffusion Tensor Tractography Grading in the Diagnosis and Prognosis Prediction of Cervical Spondylotic Myelopathy. Spine (Phila Pa 1976), 42(4)(2017), E202-e10, https://doi.org/10.1097/brs.0000000000001784
18. Nouri A, Tetreault L, Côté P, et al. Does Magnetic Resonance Imaging Improve the Predictive Performance of a Validated Clinical Prediction Rule Developed to Evaluate Surgical Outcome in Patients With Degenerative Cervical Myelopathy? Spine (Phila Pa 1976), 40(14)(2015), 1092-100, https://doi.org/10.1097/brs.0000000000000919
19. Krause T, Brunecker P, Pittl S, et al. Thalamic sensory strokes with and without pain: differences in lesion patterns in the ventral posterior thalamus. J Neurol Neurosurg Psychiatry, 83(8)(2012), 776-84, https://doi.org/10.1136/jnnp-2011-301936
20. Walton KD, Llinás RR. Frontiers in Neuroscience Central Pain as a Thalamocortical Dysrhythmia: A Thalamic Efference Disconnection? In: Kruger L, Light AR, editors. Translational Pain Research: From Mouse to Man. Boca Raton (FL): CRC Press/Taylor & Francis Copyright © 2010 by Taylor and Francis Group, LLC.; 2010.
21. Wang G, Thompson SM. Maladaptive homeostatic plasticity in a rodent model of central pain syndrome: thalamic hyperexcitability after spinothalamic tract lesions. J Neurosci, 28(46)(2008), 11959-69, https://doi.org/10.1523/jneurosci.3296-08.2008
22. Hsieh JC, Belfrage M, Stone-Elander S, et al. Central representation of chronic ongoing neuropathic pain studied by positron emission tomography. Pain, 63(2)(1995), 225-36, https://doi.org/10.1016/0304-3959(95)00048-w
23. Zhou F, Gong H, Liu X, et al. Increased low-frequency oscillation amplitude of sensorimotor cortex associated with the severity of structural impairment in cervical myelopathy. PLoS One, 9(8)(2014), e104442, https://doi.org/10.1371/journal.pone.0104442
24. Endo T, Spenger C, Tominaga T, et al. Cortical sensory map rearrangement after spinal cord injury: fMRI responses linked to Nogo signalling. Brain, 130(Pt 11)(2007), 2951-61, https://doi.org/10.1093/brain/awm237
25. Chen S, Wang Y, Wu X, et al. Degeneration of the Sensorimotor Tract in Degenerative Cervical Myelopathy and Compensatory Structural Changes in the Brain. Front Aging Neurosci, 142022), 784263, https://doi.org/10.3389/fnagi.2022.784263
26. Henderson LA, Gustin SM, Macey PM, et al. Functional reorganization of the brain in humans following spinal cord injury: evidence for underlying changes in cortical anatomy. J Neurosci, 31(7)(2011), 2630-7, https://doi.org/10.1523/jneurosci.2717-10.2011

27. Ghosh A, Haiss F, Sydekum E, et al. Rewiring of hindlimb corticospinal neurons after spinal cord injury. Nat Neurosci, 13(1)(2010), 97-104, https://doi.org/10.1038/nn.2448
28. Freund P, Wheeler-Kingshott CA, Nagy Z, et al. Axonal integrity predicts cortical reorganisation following cervical injury. J Neurol Neurosurg Psychiatry, 83(6)(2012), 629-37, https://doi.org/10.1136/jnnp-2011-301875
29. Cook LL, Foster PJ, Mitchell JR, et al. In vivo 4.0-T magnetic resonance investigation of spinal cord inflammation, demyelination, and axonal damage in chronic-progressive experimental allergic encephalomyelitis. J Magn Reson Imaging, 20(4)(2004), 563-71, https://doi.org/10.1002/jmri.20171
30. Cheung G, Gawel MJ, Cooper PW, et al. Amyotrophic lateral sclerosis: correlation of clinical and MR imaging findings. Radiology, 194(1)(1995), 263-70, https://doi.org/10.1148/radiology.194.1.7997565
31. Kuang C, Zha Y. Abnormal intrinsic functional activity in patients with cervical spondylotic myelopathy: a resting-state fMRI study. Neuropsychiatr Dis Treat, 152019), 2371-83, https://doi.org/10.2147/ndt.S209952

Figures

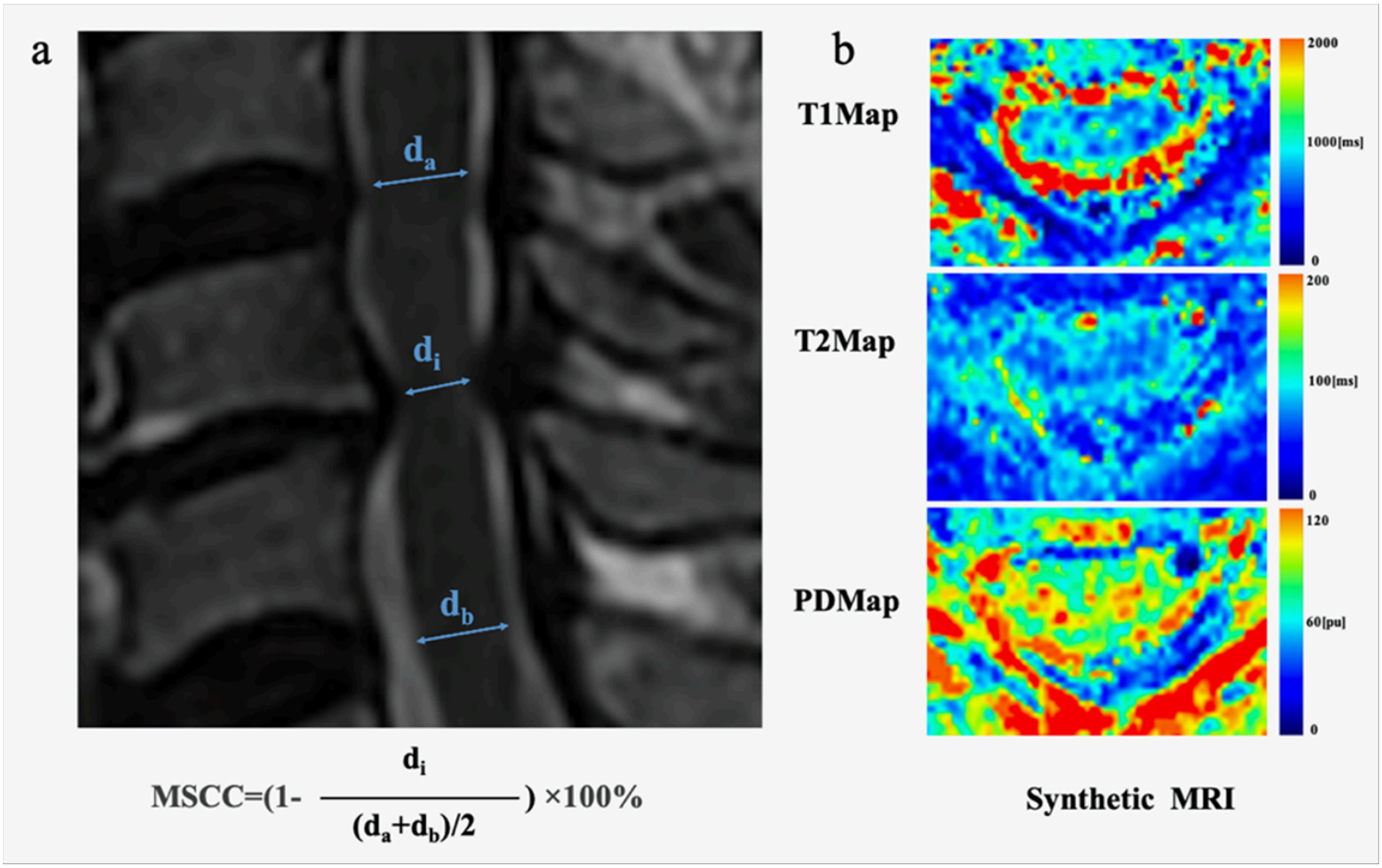

Figure 1

a: Schematic for calculating the maximum spinal cord compression (MSCC) ratio. d_i = anteroposterior diameter of the spinal cord at maximal compression level (MCL), d_a= anteroposterior diameter of the spinal cord at non-compressed level from above MCL; d_b= anteroposterior diameter of the spinal cord at non-compressed level from below MCL. b: Representative synthetic MRI colormaps (T1, T2, and PD) of the cervical spinal cord.

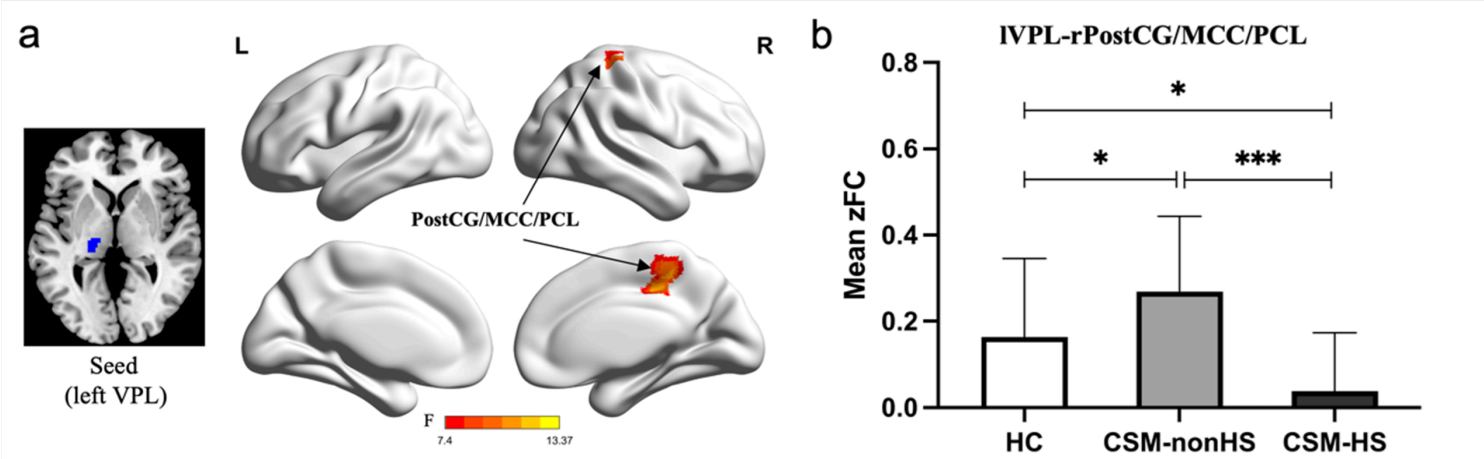

Figure 2

Voxel-wise analysis and group comparison of left ventral posterolateral nuclei (VPL) functional connectivity (zFC). a: Brain regions with significant between-group differences (one-way ANOVA, cluster-level FWE corrected, p<0.05; voxel-wise p<0.001); b: Post-hoc analysis of the mean zFC extracted from significant cluster. Connectivity was increased in the CSM-nonHS group but decreased in the CSM-HS group compared to healthy controls (HCs). * P < 0.05; ** P < 0.01; *** P < 0.001. CSM-nonHS: CSM patients without T2-hyperintensity; CSM-HS: CSM patients with T2-hyperintensity. rPostCG: right precentral gyrus; MCC: middle cingulate cortex; PCL: paracentral lobule.

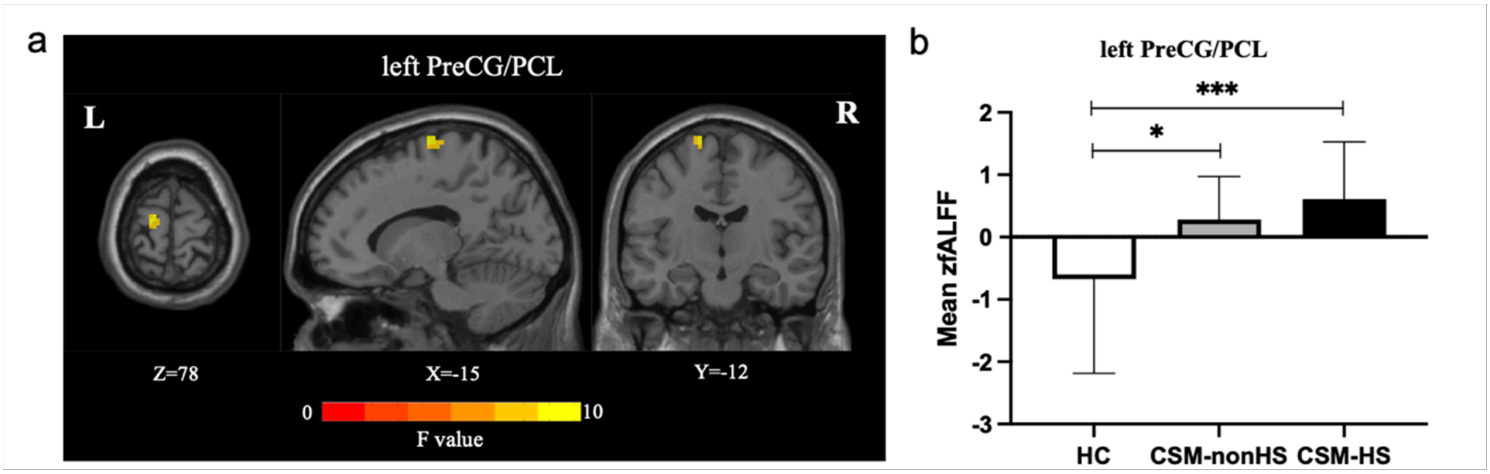

Figure 3

Voxel-wise analysis and group comparisons of z-scored Fractional Amplitude of Low-Frequency Fluctuations (zfALFF). a: Brain regions with significant between-group differences (one-way ANOVA,

cluster-level FWE corrected, p<0.05; voxel-wise p<0.001); b: Post-hoc analysis of the mean zfALFF extracted from the significant cluster. Local zfALFF values were increased in both CSM subgroups compared to HCs. * P < 0.05; ** P < 0.01; *** P < 0.001. PreCG: precentral gyrus; PCL: paracentral lobule.

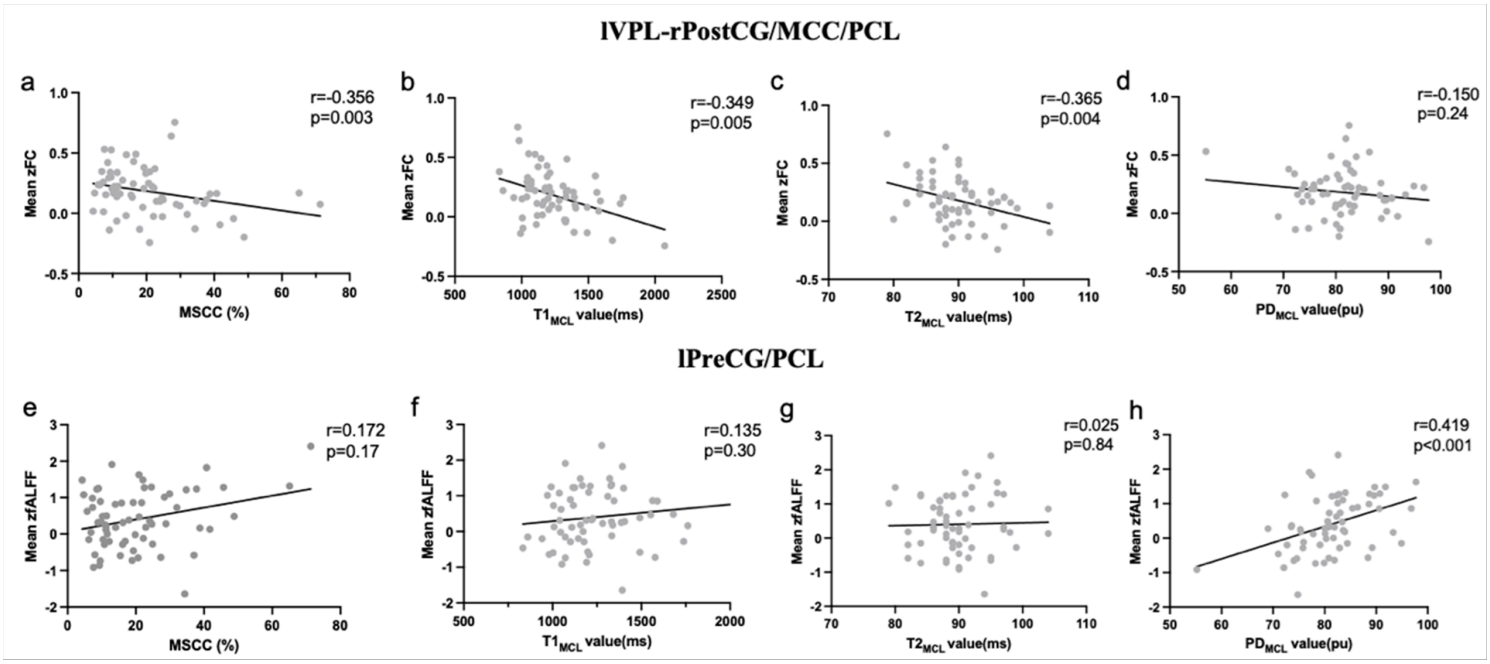

Figure 4

Correlation between fMRI metrics and quantitative spinal cord parameters at the maximum compression level (MCL) in CSM patients: a-c: Mean VPL-sensory cortex zFC values negatively correlated with $T1_{MCL}$, $T2_{MCL}$ and MSCC values. d: Mean zFC values showed no correlation with PD_{MCL} values. e-g: Mean motor cortex zfALFF values showed no significant correlation with $T1_{MCL}$, $T2_{MCL}$ and MSCC values. H: Mean zfALFF values positively correlated with PD_{MCL} values.

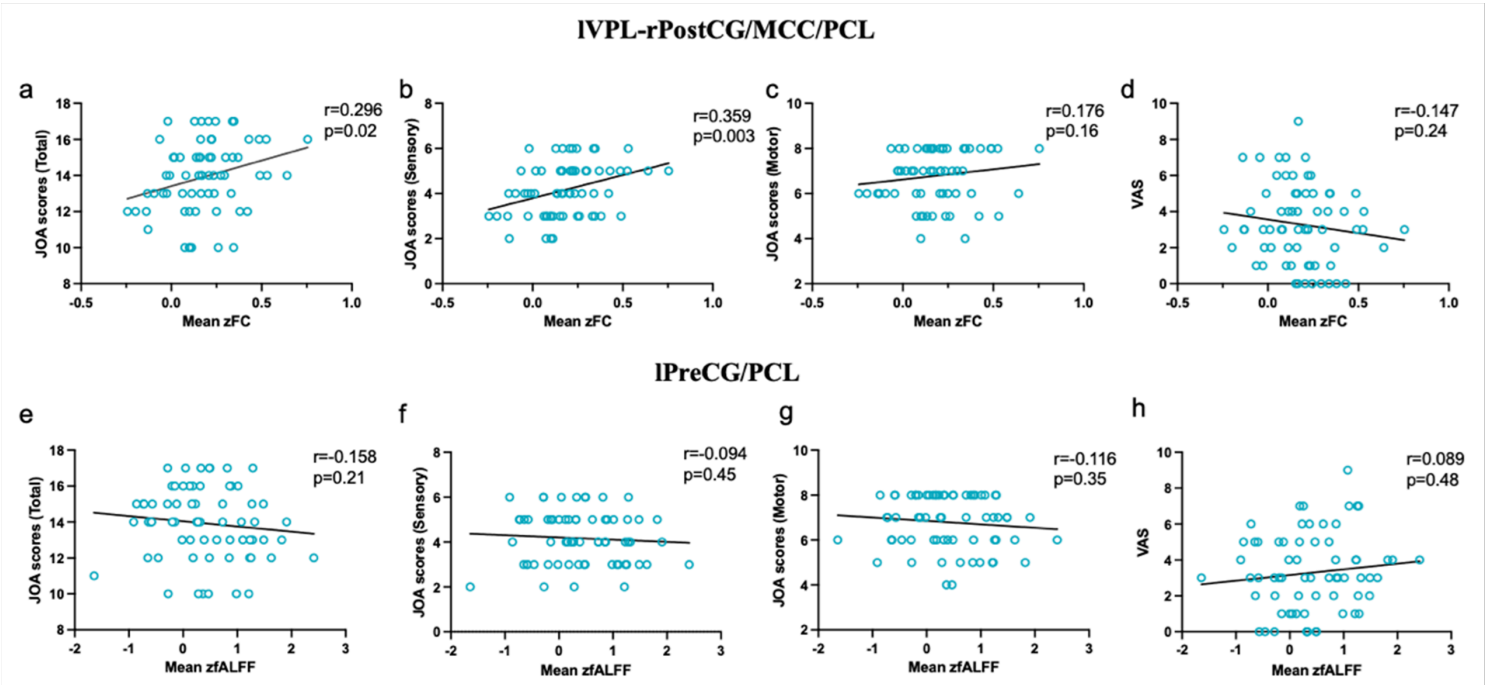

Figure 5

Correlation between fMRI metrics and clinical scores in CSM patients: a-b: Mean VPL-sensory cortex zFC values positively correlated with the total JOA scores and JOA sensory subscores. c-d: Mean zFC values showed no significant correlation with JOA motor subscores and VAS scores. e-h: Mean motor cortex zfALFF values showed no significant correlation with JOA and VAS scores.